SIN-CHN
SCIENTIFIC PRESS PTE.LTD.

Molecular & Cellular Biomechanics 2024, 21, 166.
https://doi.org/10.62617/mcb.v21.166

Article

Utilizing porous carbon composites based on biomass for lithium battery negative electrodes

Yi Chen[1], Aiwu Tang[2,*]

[1] School of Intelligent Manufacturing and Architectural Engineering, Yongzhou Vocational Technical College, Yongzhou 425000, China
[2] School of Information Engineering, Yongzhou Vocational Technical College, Yongzhou 425000, China
*** Corresponding author:** Aiwu Tang, yzzyxytangaiwu@163.com

CITATION

Chen Y, Tang A. Utilizing porous carbon composites based on biomass for lithium battery negative electrodes. Molecular & Cellular Biomechanics. 2024; 21: 166. https://doi.org/10.62617/mcb.v21.166

ARTICLE INFO

Received: 28 May 2024
Accepted: 16 July 2024
Available online: 12 August 2024

Abstract: This work used high-temperature calcination techniques along with basic chemical processing to produce a range of porous carbon compounds from biomass. After that, these substances were employed as anodes in lithium-ion batteries. The first hard carbon was produced via the dehydration reaction of strong sulfuric acid with sucrose (R-HC), then annealing in an NH_3Ar environment was used to obtain the nitrogen-doped porous hard carbon (N-HC). Because N-HC has a high interlayer spacing (ca. 0.39 nm) and an abundant ultra-microporous structure (pore size < 0.75 nm), the lithium-ion diffusion coefficient in N-HC can reach up to 9.0×10^{-8} $cm^2.s^{-1}$. The obtained porous carbon compounds contain a rich pore structure, many functional groups, and a high specific surface area, according to the results. Following their application to the anode of lithium-ion batteries, they demonstrate favorable cycle stability and electrochemical performance. Furthermore, a detailed investigation into the kinetic characteristics of the lithium-ion diffusion behavior in the electrodes revealed that the porous carbon materials' electrodes exhibited greater surface diffusion behavior for Li^+.

Keywords: biomass-based porous carbon materials; lithium-ion battery; anode; morphological characterization; electrochemical performance

1. Introduction

Batteries, a vital tool for energy conversion and storage, are becoming more and more significant in a variety of disciplines as human society and science and technology advance [1]. For energy storage systems, electric vehicles, and mobile devices, lithium-ion batteries are the recommended battery type due to its high energy density and environmental friendliness [2]. However, researchers have been looking into novel electrode materials and structural designs in an effort to accommodate the growing need for electrical energy as well as to enhance the performance and dependability of batteries [3].

Because of its excellent chemical stability, tunable microstructure, and outstanding electrical conductivity, in recent decades, researchers have focused a lot of attention on carbon materials. Given their vast surface area, abundance of active sites, and favorable electron transport properties, porous carbon compounds in particular are considered to be attractive candidates for electrode materials. Additionally, the process of turning biomass into porous carbon compounds has garnered a lot of interest for its potential use in the energy sector as a plentiful and sustainable source of carbon [4].

Current research indicates that biomass-based porous carbon composites have a promising future as anode materials for lithium batteries. Several scholars have investigated the electrochemical behavior of porous carbon materials in lithium-ion

batteries and documented their synthesis using a range of biomass sources [5]. Sources of biomass and techniques of preparation: Numerous scientists have tried to create porous carbon composites by utilizing different biomass sources, like lignin, cellulose, and wood fibers, then carbonizing, charring, and activating them. For instance, Thota SP [6] used chemical activation and high-temperature carbonization to transform peanut shells into carbon materials with a large number of porous structures, after that, they were used as electrode materials in lithium-ion battery anodes. Many studies have been conducted on the microstructure and electrochemical properties of porous carbon composites based on biomass. For example, X-ray diffraction (XRD), transmission electron microscopy (TEM), scanning electron microscopy (SEM), and specific surface area analysis (BET) were used to identify the pore structure, crystal structure, and surface morphology of the materials. In the meantime, electrochemical testing was used to assess key metrics such the materials' capacity retention, multiplicity performance, and cycling stability [7–12]. Porous carbon composites based on biomass have demonstrated strong electrochemical performance and cycling stability in lithium battery anodes, according to several research. Because of their huge specific surface area and availability of active areas, these materials can extend the cycle life of the battery and accelerate the rate at which lithium ions embed and dembedding [8–13].

As a result, among other technologies, they are thought to be a viable electrode material for use in lithium-ion batteries, sodium-ion batteries, and supercapacitors. While biomass-based porous carbon composites exhibit encouraging potential for use in lithium battery anodes, certain obstacles remain to be addressed. These include the enhancement of material preparation efficiency, the investigation of the connection between performance and structure, and the safety and stability of cycling.

To create anode materials for lithium batteries with better performance, new approaches to material preparation and design are being explored. The optimization of preparation techniques, the investigation of the connection between material structure and performance, and the stability and dependability in real-world applications are some of the remaining research problems, though. This work investigates the usage of porous carbon composites based on biomass in lithium battery anodes. The production process, structural properties, and electrochemical performance of porous carbon composites obtained from biomass in lithium-ion battery anodes are all to be investigated in this work. This study is important because it offers fresh concepts and approaches for creating lithium batteries that are both affordable and highly effective. The work methodically examines the use of material-based porous carbon composites in the anode of lithium batteries, combining extensive material characterization with electrochemical performance testing. Elevated electrochemical performance and good cycling stability are anticipated from electrode materials that are optimized in terms of their structural design and material preparation. This will offer crucial technical assistance for enhancing lithium battery performance and promoting their use.

2. Experimentation

2.1. Sample preparation

5.0 g of analytically pure sucrose were removed, and a 250 mL beaker was filled

with 1 mL of deionized water. Subsequently, 9.0 mL of concentrated sulfuric acid (95%–98%) was added drop by drop to the sucrose while shaking and using a pipette gun. The sucrose turned from white to yellow to brown to black foam when the strong sulfuric acid was added little by little. Following the collection of the black foam, the filtrate was neutralized by washing it with deionized water, freezing it in liquid nitrogen, and lyophilizing it to produce R-HC. To obtain the N-HC sample, the R-HC was heated in a tube furnace to 800 ℃ at a rate of 5 °C per minute. It was then maintained in an environment of NH_3/Ar (1:1, v/v/v) for 6 hours before being cooled to room temperature.

2.2. Sample characterization

Using FESEM (Field emission transmission electron microscope) (Hitachi, Japan) and FETEM (JEOL, Japan) with accelerating voltages of 2 kV and 200 kV, respectively, sample morphology and microstructure were examined [14]. A Raman spectrometer (λ = 532 nm, P = 10 mW) was used to characterize the defect content of the samples. XPS (Thermo, US) was used to characterize the samples. The materials' chemical components and valence states were assessed by the use of Thermo Scientific XPS (US) with monochromatic Al $K\alpha$ (hv = 1486.6 eV), 150 W of power, and a 500 μm X-ray beam spot lastly, utilizing a fully automated gas adsorption apparatus (Quantachrome, US) with isothermal carbon dioxide adsorption and desorption of nitrogen at room temperature, the pore size distributions and specific surface areas of the samples were examined.

2.3. Half-cell assembly

After being combined in a mass ratio of 75:15:10 with polyvinylidene fluoride (PVDF) and Cochin black (EC-600JD), after being crushed into a slurry and placed on copper foil, the active ingredients (R-H, N-HC, and lithium iron phosphate, or LFP) were left to dry at 80 °C for 12 hours. With a mass loading of 1.0–1.5 mg.cm^{-2} for R-HC and 1.0–1.5, 2.0–2.5, and 2.8–3.5 mg.cm^{-2} for N-HC, respectively, the electrode sheets were cut into 10 mm diameter electrodes. A 2032-type button half-cell was assembled in a glove box (H_2O and O_2 concentrations less than 10–6) using lithium foil as the diaphragm, 1.0 M LiPF6 as the electrolyte, and polypropylene (Celgard 2400) as the reference and counter electrodes. Press the half-cell button.

2.4. Electrochemical testing

R-HC, N-HC, and LFP half-cells as well as N-HC//LFP full-cells were subjected to electrochemical impedance spectroscopy using a CHI 760E electrochemical workstation [15]. Cyclic voltammetric curve testing was performed on the LFP half-cells and N-HC/LFP full-cells between 2.5 and 4.5 V and 2.5 and 4.2 V, respectively. In cyclic voltammetric curves, R-HC and N-HC were evaluated as negative electrodes throughout a voltage range of 0.001–3.000 V with a scan rate of 1–10 mV.s^{-1}. There was a scan rate range of 1 to 10 mV-s-3. Performance tests for multiplication, cycle stability, and constant-current charge/discharge were conducted using a Land CT 2001 A test system. Instead of using the mass of the conductive agent and binder, the mass of the active material in the electrodes was used to compute the specific capacity,

energy density, and power density.

3. Findings and conversation

3.1. Material morphology and structure analysis

Images of the R-HC and N-HC samples captured using transmission electron microscopy (FETEM) and field emission scanning electron microscopy (FESEM) are displayed in **Figure 1** [16]. A dispersion of small but big pores with a typical amorphous carbon structure can be seen in the R-HC sample (**Figure 1a–c**). Pores of varying diameters are randomly scattered on the surface of the N-HC sample (**Figure 1d**), which may be the result of gases produced during the calcination of R-HC from the breakdown of functional groups containing oxygen. After annealing at 800 °C, the N-HC samples (**Figure 1e,f**) still had an amorphous carbon structure, but they now had randomly dispersed curved lamellae with a 0.39 nm layer spacing.

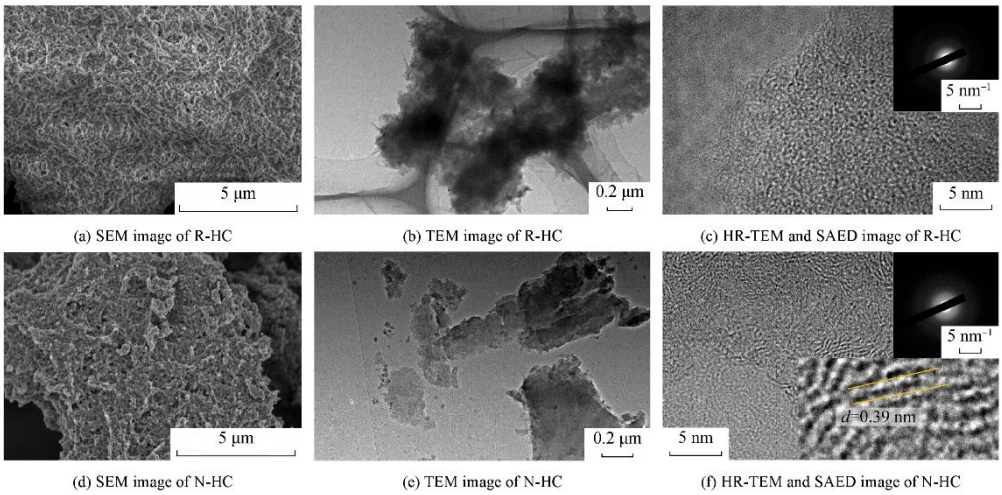

Figure 1. Morphological characterization of R-HC and N-HC samples.

Figure 2 shows the results of the tests that were conducted on the R-HC and N-HC samples using gas adsorption, including X-ray photoelectron spectroscopy (XPS), Raman spectroscopy, and X-ray diffraction (XRD). The characteristic peak of (002) in the R-HC sample's XRD pattern (**Figure 2a**) is located at $2\theta = 20.5°$, which indicates that the corresponding layer spacing is 0.43 nm. In contrast, the N-HC sample's characteristic peak has shifted to $2\theta = 23.1°$, and the corresponding layer spacing decreases to 0.39 nm. On the other hand, the N-HC sample's XRD pattern showed more prominent peaks in the (101) facet spacing, which is most likely due to the sample's higher crystallinity during the annealing process.

The Raman spectra of the two samples showed that their characteristic peaks were located at 1346 cm^{-3} and 1589 cm^{-3} (**Figure 2b**). The two samples' estimated ID/IG values of 0.83 and 1.06 indicate that the N-HC sample had more flaws than the other. Gas adsorption tests revealed that the specific surface areas of R-HC and N-HC were, respectively, 1581.7 $m^2.g^{-1}$ and 60.2 $m^2.g^{-1}$ (**Figure 2c**). N-HC was largely defined by a microporous structure, whereas R-HC was primarily mesoporous (**Figure 2d**).

The calculated ID/IG values for the R-HC and N-HC samples were 1.06 and 0.83,

respectively, indicating that the N-HC sample was more flawed. As seen in **Figure 2e**, the N-HC samples were primarily microporous, with pore sizes of 0.645 $cm^3.g^{-1}$; however, the R-HC samples likewise exhibited microporous characteristics, with pore volumes of 0.654 $cm^3.g^{-1}$. The nitrogen isothermal adsorption/desorption experiments yielded specific surface areas of 1581.7 $m^2.g^{-1}$ for the R-HC sample and 60.2 $m^2.g^{-1}$ for the N-HC sample. Micropores (less than 2 nm) with a pore volume of 0.645 $cm^3.g^{-1}$ predominate in N-HC. **Figure 2f** revealed that N-HC contains 8.03% nitrogen atoms in addition to graphitized, pyridine, and pyrrole nitrogen.

In N-HC, the volume and specific surface area of microporous materials were 0.206 $cm^3.g^{-1}$ and 784.8 $m^2.g^{-1}$ respectively, which were 2.8 and 2.9 times greater than those of the R-HC sample, as indicated in **Figure 2d–f**. The N-HC sample has a large amount of ultra-microporous structure (< 0.75 nm), as can be seen from the above data, and the R-HC sample's ultra-microporous volume is just 0.043 $cm^3.g^{-1}$, compared to its 0.167 $cm^3.g^{-1}$ ultra-microporous volume.

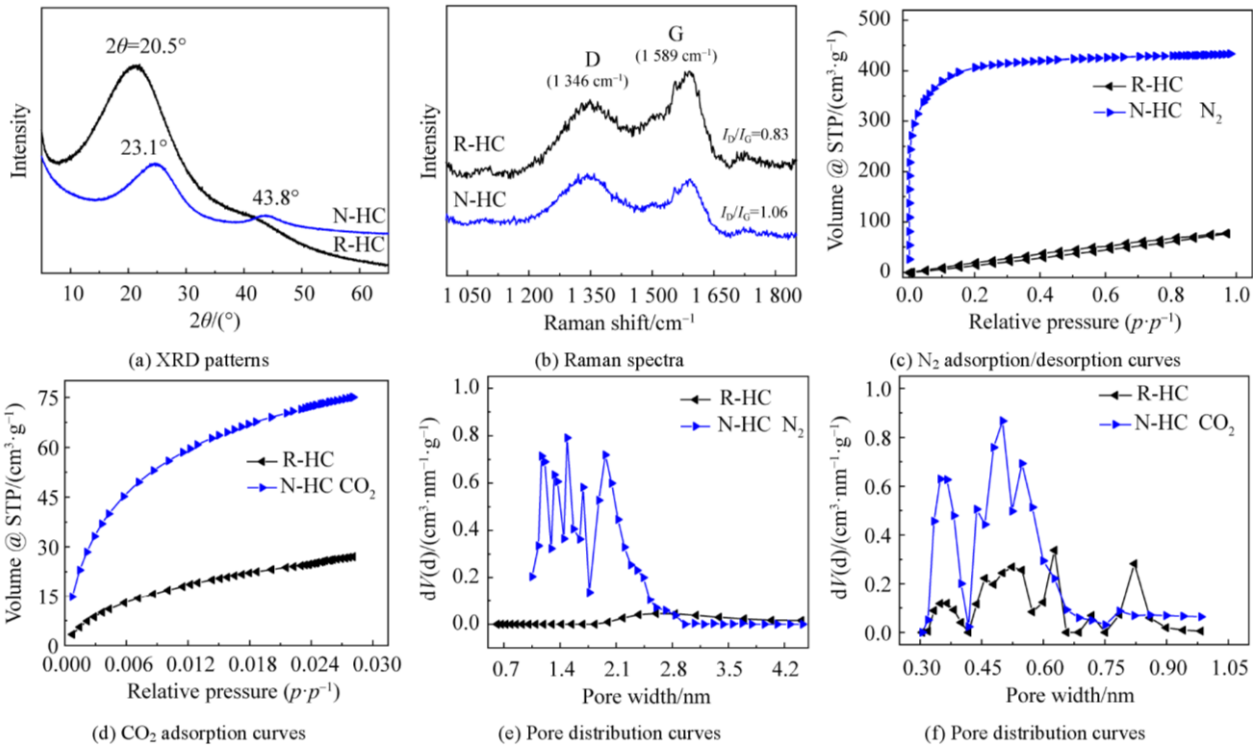

Figure 2. Structural characterization of R-HC and N-HC samples.

As illustrated in **Figure 3a**, N-HC has 8.03% (mole fraction) more nitrogen atoms than R-HC in addition to carbon and oxygen. The contents of C-sp^3 and C-sp^2 in the R-HC samples were 47.9% and 25.3%, respectively, as can be seen in **Figure 3b**. In the R-HC and N-HC samples (**Figure 3c–f**), the percentage of oxygen atoms is 25.4% and 17.3%, respectively, with the majority of these atoms being in the O-C form. In contrast, the contents of C-sp^3 and C-sp^2 in the N-HC samples were 37.1% and 31.9% respectively, and the elevated contents of C-sp2 in the N-HC samples were consistent with the XRD characterization results, as can be seen in **Figure 3e**. **Figure 3d** shows the N 1s high-resolution spectra of the N-HC sample. It demonstrates that the amounts of nitrogen in pyrrole (400.0 eV) and pyridine (398.2 eV), and graphitized nitrogen

(402.9 eV) are, in that order, 29.6%, 52.5%, and 17.9%. Prior research has demonstrated that while the graphitized nitrogen structure increases the electrical conductivity of carbon materials, electrochemically active pyridine and pyrrole nitrogens add to the lithium storage capacity [14].

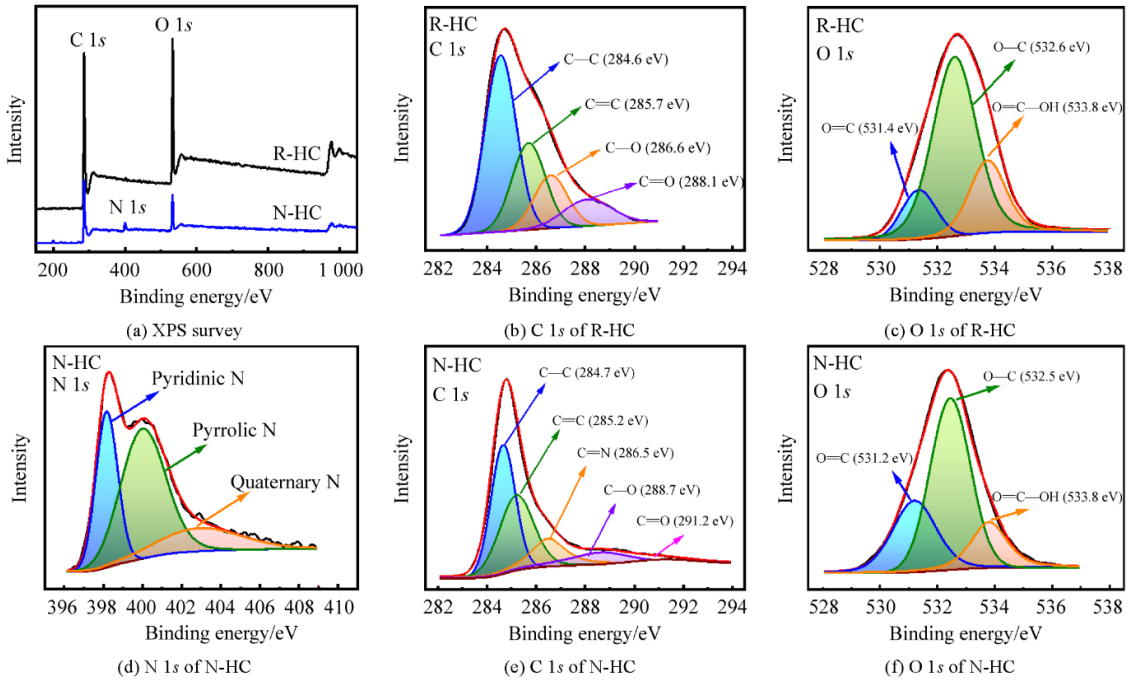

Figure 3. XPS spectra of R-HC and N-HC samples.

3.2. Electrochemical performance analysis

The R-HC and N-HC electrodes' electrochemical performance is displayed in **Figure 4**. The wider region encircled by the N-HC electrode's curve in **Figure 4a**, suggests that the electrode has a greater capacity to store lithium. The electrochemical impedance spectra of the N-HC and R-HC electrodes were fitted, as shown in **Figure 4b**, to ascertain the N-HC and R-HC electrodes' respective electrode charge transfer resistance (R_{ct}) values of 15.8 Ω and 113.8 Ω. The smaller R_{ct} of the N-HC electrode suggests a faster electron transfer capability. As seen in **Figure 4c**, the results of cyclic voltammetry curve testing at various scanning speeds were analyzed using Spss [14,16]. In order to look into the kinetic characteristics of Li^+ in the electrodes, the N-HC electrodes have greater surface diffusion behaviors of Li^+ than the R-HC electrode, given that their corresponding *b* values are 0.68 and 0.77.

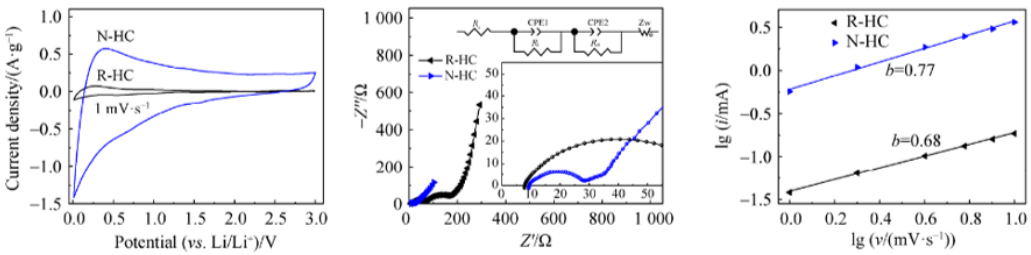

Figure 4. Characteristics of R-HC and N-HC electrodes' electrochemistry.

4. Conclusion

In this study, porous carbon composites based on biomass were prepared and applied to lithium battery anodes, yielding a number of significant experimental outcomes. First, we show how to successfully prepare biomass-based porous carbon composites with good structure and characteristics for lithium-ion batteries by providing a complete description of sample preparation, characterization, and half/full cell assembly. Secondly, upon examination of the material's shape, structure, and electrochemical characteristics, we discovered that the porous carbon composites derived from biomass have superior electrochemical capabilities, greater specific surface area compared to conventional carbon composites, and more structural flaws. The N-HC samples, in particular, demonstrate their significant potential in lithium-ion battery anodes due to their improved surface diffusion behavior, faster electron transfer rate, and larger lithium storage capacity.

Even with the advancements this study has made, there are still certain unanswered questions and potential future research areas. Initially, by modifying the biomass species, preparation method, and carbonization conditions, the structure and characteristics of biomass-based porous carbon composites can be further enhanced to increase their performance in lithium-ion battery applications. Secondly, further investigation into the stability and cycle life of biomass-based porous carbon composites can be conducted to determine their viability for large-scale commercial applications. To increase their uses in the energy industry, biomass-based porous carbon composites can also be included into other energy conversion and storage technologies as fuel cells, sodium-ion batteries, and supercapacitors. In conclusion, a deeper comprehension of the connection between the structure and characteristics of porous carbon composites based on biomass can be achieved by combining theoretical computations with simulations. This will provide scientific direction and support for the continued optimization and application of these materials.

Author contributions: Conceptualization, YC and AT; methodology, YC; software, YC; validation, YC and AT; formal analysis, YC; investigation, YC; resources, YC; data curation, YC; writing—original draft preparation, YC; writing—review and editing, YC; visualization, YC; supervision, YC; project administration, YC; funding acquisition, AT. All authors have read and agreed to the published version of the manuscript.

Funding: 2022 Science Research Project of Hunan Provincial Department of Education "Preparation and First-principles Research of Silicon-carbon Anode Materials for high-performance lithium Batteries Based on biomass Modification" (22C1348).

Ethical approval: The study was conducted in accordance with the Declaration of Helsinki, and approved by the Institutional Review Board (or Ethics Committee) of Yongzhou Vocational Technical College (protocol code YZ20240755653 and 03/02/2024 date of approval).

Conflict of interest: The authors declare no conflict of interest.

References

1. Sun L, Gong Y, Li D, et al. Biomass-derived porous carbon materials: synthesis, designing, and applications for supercapacitors. Green Chemistry. 2022; 24(10): 3864–3894. doi: 10.1039/d2gc00099g
2. Jin C, Nai J, Sheng O, et al. Biomass-based materials for green lithium secondary batteries. Energy & Environmental Science. 2021; 14(3): 1326–1379. doi: 10.1039/d0ee02848g
3. Ashok Kumar SS, Bashir S, Pershaanaa M, et al. A review on the recent progress of the plant-based porous carbon materials as electrodes for high-performance supercapacitors. Journal of Materials Science. 2023; 58(15): 6516–6555. doi: 10.1007/s10853-023-08413-7
4. Karaman C, Karaman O, Atar N, et al. Sustainable electrode material for high-energy supercapacitor: biomass-derived graphene-like porous carbon with three-dimensional hierarchically ordered ion highways. Physical Chemistry Chemical Physics. 2021; 23(22): 12807–12821. doi: 10.1039/d1cp01726h
5. Chen Q, Tan X, Liu Y, et al. Biomass-derived porous graphitic carbon materials for energy and environmental applications. Journal of Materials Chemistry A. 2020; 8(12): 5773–5811. doi: 10.1039/c9ta11618d
6. Thota SP, Bag PP, Vadlani PV, Belliraj SK. Plant Biomass Derived Multidimensional Nanostructured Materials: A Green Alternative for Energy Storage. Engineered Science. 2022. doi: 10.30919/es8d664
7. Md Zaini MS, Anuar NF, Al-Junid SAM, et al. Agricultural biomass-based carbon cathode materials for lithium-sulfur batteries: A systematic review. Materials Science for Energy Technologies. 2023; 6: 205–225. doi: 10.1016/j.mset.2022.12.009
8. Yakaboylu GA, Jiang C, Yumak T, et al. Engineered hierarchical porous carbons for supercapacitor applications through chemical pretreatment and activation of biomass precursors. Renewable Energy. 2021; 163: 276–287. doi: 10.1016/j.renene.2020.08.092
9. Szczęśniak B, Phuriragpitikhon J, Choma J, et al. Recent advances in the development and applications of biomass-derived carbons with uniform porosity. Journal of Materials Chemistry A. 2020; 8(36): 18464–18491. doi: 10.1039/d0ta05094f
10. Li T, Zhi DD, Guo ZH, et al. 3D porous biomass-derived carbon materials: biomass sources, controllable transformation and microwave absorption application. Green Chemistry. 2022; 24(2): 647–674. doi: 10.1039/d1gc02566j
11. Cheng D, Tian M, Wang B, et al. One-step activation of high-graphitization N-doped porous biomass carbon as advanced catalyst for vanadium redox flow battery. Journal of Colloid and Interface Science. 2020; 572: 216–226. doi: 10.1016/j.jcis.2020.03.069
12. Aini Q, Irmawati Y, Karunawan J, et al. Para Grass-Derived Porous Carbon-Rich SiOx/C as a Stable Anode for Lithium-Ion Batteries. Energy & Fuels. 2023; 37(15): 11397–11405. doi: 10.1021/acs.energyfuels.3c01678
13. Wang R, Li X, Nie Z, et al. NiCo2O4 Hexagonal Nanoplates/Cornstalk-Derived Porous Carbon Composites for High-Performance Supercapacitor Electrodes. Energy & Fuels. 2022; 36(21): 13256–13265. doi: 10.1021/acs.energyfuels.2c02441
14. Bongu CS, Sharma CS. Ginger-derived hierarchical porous carbon as an anode material for potassium-ion batteries and capacitors. Materials Advances. 2024; 5(2): 632–641. doi: 10.1039/d3ma00732d
15. Fu F, Wang H, Yang D, et al. Lamellar hierarchical lignin-derived porous carbon activating the capacitive property of polyaniline for high-performance supercapacitors. Journal of Colloid and Interface Science. 2022; 617: 694–703. doi: 10.1016/j.jcis.2022.03.023
16. Li X, Luo W, Zhu K, et al. Electronic modulation of S and N co-implanted carbon as fenton-like photocatalysts for water remediation. Chemical Engineering Journal. 2023; 474: 146016. doi: 10.1016/j.cej.2023.146016